



Electrochemical and theoretical quantum approaches on the inhibition of mild steel corrosion in HCl using synthesized benzothiazine compound

K. Al Mamari^{1,4}, H. Elmsellem^{2*}, N. K. Sebbar¹, A. Elyoussfi², H. Steli⁵, M. Ellouz¹, Y. Ouzidan³, A. Nadeem¹, E. M. Essassi¹ and F. El-Hajjaji⁶

¹Laboratoire de Chimie Organique Hétérocyclique, URAC 21, Pôle de Compétences Pharmacochimie, Mohammed V University in Rabat, Faculté des Sciences, Av. Ibn Battouta, BP 1014 Rabat, Morocco.

²Laboratoire de chimie analytique appliquée, matériaux et environnement (LC2AME), Faculté des Sciences, Université Mohammed Premier, B.P. 717, 60000 Oujda, Morocco

³Laboratoire de Chimie Organique Appliquée, Université Sidi Mohamed Ben Abdallah, Faculté des Sciences et Techniques, Route d'Immouzer, BP 2202 Fes, Morocco.

⁴Department of Chemistry - Faculty of Education University of Hodiedah – Yemen.

⁵Laboratoire mécanique & énergétique, Faculté des Sciences, Université Mohammed Premier, Oujda, Maroc

⁶Laboratoire d'Ingénierie d'Electrochimie de Modélisation et Environnement (LIEME) FSDM, Université Sidi Mohammed Ben Abdallah, Fès, Morocco.

Received 31 Apr 2016, Revised 27 July 2016, Accepted 4 Aug 2016

*Corresponding author. E-mail : h.elmsellem@yahoo.fr Tél : +212670923431

Abstract

4-allyl-2H-1,4-benzothiazin-3(4H)-one (**P2**), have been synthesized, characterized by NMR spectroscopy, and tested as corrosion inhibitor for mild steel in HCl solution using potentiodynamic polarization curves and electrochemical impedance spectroscopy. Potentiodynamic polarization curve measurements showed that the investigated compound was a mixed-type inhibitor. Its inhibition efficiencies improve with concentration and reached a maximum at 10^{-3} M. Electrochemical impedance spectroscopy (EIS) studies suggested that P2 inhibit mild steel corrosion by becoming adsorbate at the metallic/electrolyte surfaces. Adsorption of the inhibitor on the mild steel surface was found to obey Langmuir's adsorption isotherm. Further, the electronic structural calculations using quantum chemical methods were found to be in a good agreement with the results of the experimental studies.

Keywords: Mild steel, 1,4-benzothiazine, EIS, Corrosion, Weight loss, Electrochemical, DFT.

1. Introduction

The study of corrosion inhibition is a very active field of research. Several classes of organic compounds are widely used as corrosion inhibitors for metals in acid environments [1–2]. Experimental means are useful to explain the inhibition mechanism but they are often expensive and time-consuming. Several quantum chemical methods and molecular modeling techniques have been performed to correlate the inhibition efficiency of the inhibitors with their molecular properties [3–4]. Using theoretical parameters helps to characterize the molecular structure of the inhibitors and to propose their interacting mechanism with surfaces [5]. Some studies have shown that the inhibition of the corrosion process is mainly described by the formation of donor–acceptor

surface complexes between free or p-electrons of an organic inhibitor, mostly containing nitrogen, sulfur or oxygen atoms, and a vacant d-orbital of a metal [6–7]. Over the years, 1,4-benzothiazine derivatives have constituted an important class of heterocycles which, even when part of a complex molecule [8], possess a wide spectrum of biological activities [9-10], due to the presence of a fold along the nitrogen sulfur axis. The biological activity of some 1,4-benzothiazine derivatives is similar to that of phenothiazines, featuring the same structural specificity [11-13]. The role of 1,4-benzothiazine in medicinal chemistry was reviewed earlier [14]. Generally, benzothiazine and derivatives have found widespread applications as analgesic [15], antibacterial [16], anticancer [17], anthelmintic [18].

The present study aimed to test new compound (**P2**) on the corrosion of mild steel in 1 M hydrochloric acid solution. Compound (**P2**) was synthesized by realizing the alkylation reaction with allyl bromide, under phase-transfer catalysis conditions using tetra n-butyl ammonium bromide (TBAB) as catalyst and potassium carbonate as base (Figure 1).

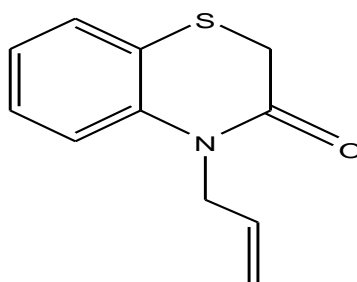


Figure 1: 4-allyl-2H-1,4-benzothiazin-3(4H)-one (**P2**)

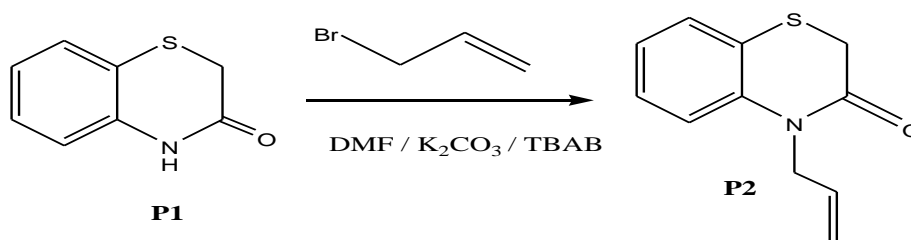
2. Experimental

2.1. Materials and solutions

The mild steel strips having a composition (wt.%) of 0.09% P, 0.01 % Al, 0.38 % Si, 0.05 % Mn, 0.21 % C, 0.05 % S and Fe balance were mechanically cut into $1.5 \times 1.5 \times 0.05 \text{ cm}^3$ dimensions for the electrochemical experiments. The surface of the specimens was abraded with emery paper grade 600 and 1200, which was then washed in deionized water, degreased ultrasonically in ethanol and acetone. The acid solutions (1.0 M HCl) were prepared by dilution of analytical reagent-grade 98 % HCl with double-distilled water. The range of concentration of P2 was 10^{-6} M to 10^{-3} M .

2.2. Synthesis of inhibitor

To a solution of 3,4-dihydro-2H-1,4-benzothiazin-3-one **P1** (6.06 mmol) in 20 ml of DMF, was added (7.27 mmol) of potassium carbonate, The mixture is stirred magnetically for 5 minutes then added 0.6 mmol of tetra-n-butylammonium bromide (TBAB) and drip (12.12 mmol) of allyl bromide, then the mixture was stirred magnetically for 24 h. After removal of salts by filtration, DMF was evaporated under reduced pressure and the residue obtained is dissolved in dichloromethane. The rest of the salts are extracted with distilled water and the mixture obtained is chromatographed on silica gel column (eluent: ethyl acetate / hexane (1/9))(**Schema 1**):



Scheme 1: Synthesis of 4-allyl-2H-1,4-benzothiazin-3(4H)-one (**P2**).

The analytical and spectroscopic data are conforming to the structure of compound formed:

(P2): Yield: 72%; **mp:** brown oil; **RMN¹H (DMSO-d₆) δ ppm:** 7.39-6.98 (m, 4H, H_{ar}), 5.82 (m, 1H, CH=CH₂), 5.08 (m, 2H, CH=CH₂), 4.54 (m, 2H; NCH₂), 3.52 (s, 2H, S-CH₂). **RMN¹³C (DMSO-d₆) δ ppm:** 165.0 (C=O), 123.4, 139.8 (Cq), 118.6, 124.0, 127.7, 128.4 (CH_{ar}), 133.4 (CH=CH₂), 116.2 (CH=CH₂), 46.7 (NCH₂), 30.7 (SCH₂).

Mild steel corrosion behavior in 1 M HCl was investigated in the absence and the presence of 1,4-benzothiazine derivative (P2) with the help of weight loss and electrochemical techniques. It was seen that mild steel dissolution rate was very high in 1 M HCl alone but presence of inhibitor significantly decreased the corrosion rate of mild steel.

2.3. Electrochemical measurements

The electrochemical study was carried out using a potentiostat PGZ100 piloted by Voltmaster soft-ware. This potentiostat is connected to a cell with three electrode thermostats with double wall. A saturated calomel electrode (SCE) and platinum electrode were used as reference and auxiliary electrodes, respectively. Before all experiments, the potential was stabilized at free potential during 30 min. The solution test is there after de-aerated by bubbling nitrogen. The electrochemical impedance spectroscopy (EIS) measurements are carried out with the electrochemical system, which included a digital potentiostat model Voltalab PGZ100 computer at Ecorr after immersion in solution without bubbling. After the determination of steady-state current at a corrosion potential, sine wave voltage (10 mV) peak to peak, at frequencies between 100 kHz and 10 mHz are superimposed on the rest potential. Computer programs automatically controlled the measurements performed at rest potentials after 0.5 hour of exposure at 308 K. The impedance diagrams are given in the Nyquist representation. Experiments are repeated three times to ensure the reproducibility.

2.4. Quantum chemical calculations

Quantum chemical calculations are used to correlate experimental data for inhibitors obtained from different techniques (viz., electrochemical and weight loss) and their structural and electronic properties. According to Koop man's theorem [19], E_{HOMO} and E_{LUMO} of the inhibitor molecule are related to the ionization potential (I) and the electron affinity (A), respectively. The ionization potential and the electron affinity are defined as I = -E_{HOMO} and A = -E_{LUMO}, respectively. Then absolute electronegativity (χ) and global hardness (η) of the inhibitor molecule are approximated as follows [20]:

$$\chi = \frac{I+A}{2}, \quad \chi = -\frac{1}{2}(E_{HOMO} + E_{LUMO}) \quad (1)$$

$$\eta = \frac{I-A}{2}, \quad \eta = -\frac{1}{2}(E_{HOMO} - E_{LUMO}) \quad (2)$$

Where I = -E_{HOMO} and A = -E_{LUMO} are the ionization potential and electron affinity respectively.

The fraction of transferred electrons ΔN was calculated according to Pearson theory [21]. This parameter evaluates the electronic flow in a reaction of two systems with different electronegativities, in particular case; a metallic surface (Fe) and an inhibitor molecule. ΔN is given as follows:

$$\Delta N = \frac{\chi_{Fe} - \chi_{inh}}{2(\eta_{Fe} + \eta_{inh})} \quad (3)$$

Where χ_{Fe} and χ_{inh} denote the absolute electronegativity of an iron atom (Fe) and the inhibitor molecule, respectively; η_{Fe} and η_{inh} denote the absolute hardness of Fe atom and the inhibitor molecule, respectively. In order to apply the eq. 3 in the present study, a theoretical value for the electronegativity of bulk iron was used χ_{Fe} = 7 eV and a global hardness of η_{Fe} = 0, by assuming that for a metallic bulk I = A because they are softer than the neutral metallic atoms [21].

The electrophilicity has been introduced by Sastri et al. [22], is a descriptor of reactivity that allows a quantitative classification of the global electrophilic nature of a compound within a relative scale. They have

proposed the ω as a measure of energy lowering owing to maximal electron flow between donor and acceptor and ω is defined as follows.

$$\omega = \frac{\chi^2}{2\eta} \quad (4)$$

The Softness σ is defined as the inverse of the η [23]

$$\sigma = \frac{1}{\eta} \quad (5)$$

Using left and right derivatives with respect to the number of electrons, electrophilic and nucleophilic Fukui functions for a site k in a molecule can be defined [24].

$$f_k^+ = P_k(N+1) - P_k(N) \quad \text{for nucleophilic attack} \quad (6)$$

$$f_k^- = P_k(N) - P_k(N-1) \quad \text{for electrophilic attack} \quad (7)$$

$$f_k^{\cdot} = [P_k(N+1) - P_k(N-1)]/2 \quad \text{for radical attack} \quad (8)$$

where, $P_k(N)$, $P_k(N+1)$ and $P_k(N-1)$ are the natural populations for the atom k in the neutral, anionic and cationic species respectively.

3. Results and discussion

3.1. Electrochemical impedance spectroscopy (EIS) measurements

3.1.1. Effect of inhibitor concentration

EIS measurements were carried out to investigate the inhibition effect of P2 inhibitor as well as the kinetics of corrosion reaction process. Figures 2 and 3 shows the impedance responses of the mild steel in 1 M HCl in the absence and presence of different concentrations of P2 represented in (9) Nyquist, Bode modulus and Phase angle formats (10). Similar plots for mild steel 1 M HCl system without and with P2. The shapes of the Nyquist plots in the absence and presence of P2 in the investigated environment are similar indicating that, the introduction of the investigated compound into the corrosive medium did not alter the mechanism of the corrosion process.

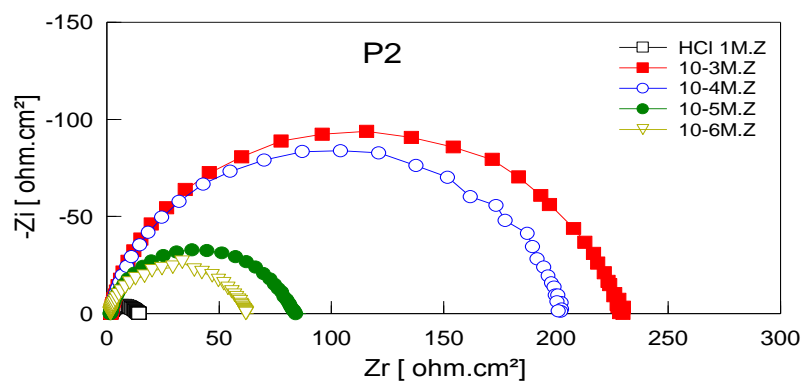


Figure 2: Nyquist diagram for mild steel in 1 M HCl in the absence and presence of P2.

The Nyquist plots are characterized by one capacitive semicircle showing that the corrosion process was charge transfer controlled [25]. The single capacitive semicircle loop corresponds to one time constant in the Bode plots. The diameter of the semicircle is observed to increase as the inhibitor concentration increased which can be related to the increase of surface coverage of inhibitive molecules on mild steel surface [26]. For the description of a frequency independent phase shift between an applied alternating potential and its current response, a constant phase element (CPE) is used instead of double layer capacitance (C_{dl}). The CPE is defined by the following expression [27, 28]:

$$Z_{CPE} = 1/A(j\omega)^n \quad (9)$$

Where $Z_{(CPE)}$, impedance of CPE; A , a proportional factor; ω , angular frequency; J , an imaginary number; n is the CPE exponent which can be used as a gauge of the heterogeneity or roughness of the surface [29]. If the

electrode surface is homogeneous and plane, the exponential value (n) becomes equal to 1 and the metal–solution interface acts as a capacitor with regular surface, i.e. when n = 1, A = capacitance. The lower value of n (Table 1) for 1 M HCl medium indicated surface inhomogeneity resulted from roughening of metal surface due to corrosion. Addition of P2 inhibitor (10⁻³ mol/l) increased in value from 0.88 to 0.93 indicating reduction of surface inhomogeneity due to the adsorption of inhibitor molecules.

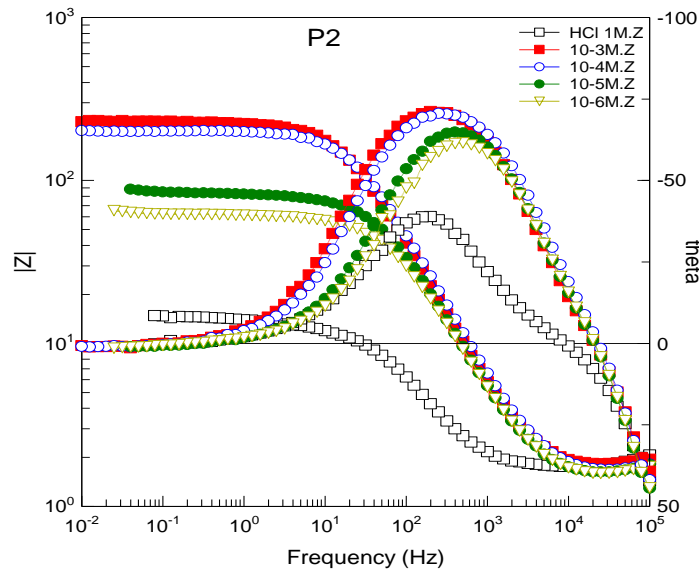


Figure 3: Bode and phase plots of mild steel in 1M HCl at different concentrations of P2 at 308 K.

From Bode modulus and phase angle plots (Figure 3), an increase in the absolute impedance at low frequencies in Bode modulus plots could be observed. This confirms the higher protection with increasing concentration of inhibitor, which is related to the adsorption of P2 on the mild steel surface.

Also a continuous increase in the phase angle shift and a new phase angle shift at higher frequency range with increasing concentration of P2 could be observed. Recently, Tan et al. and Sakunthala et al. [30, 31] have reported that, the phase angle shift is due to the formation of the protective layer on the electrode surface by inhibitor molecules which change the electrode interfacial structure. Based on the EIS data, the double-layer capacitance (C_{dl}) and the inhibition efficiency ($E_{R_{ct}}\%$) were calculated using the following equations (10):

$$E_{R_{ct}}\% = \frac{R_{ct}/inh - R_{ct}}{R_{ct}/inh} * 100 \quad (10)$$

where R_{ct}/inh and R_{ct} are the charge transfer resistance values with and without inhibitor, respectively.

Figure 4 show the comparison of experimental EIS data and the simulated spectrum, using the **Zview** impedance fitting program for mild steel samples immersed in 1 M HCl and in the presence of 10⁻³ M P2. A good fit was obtained with the model used for all experimental data. The equivalent circuit used in the present work is shown in Figure 5. In this circuit, R_s is the solution resistance, R_{ct} is the charge transfer resistance, and CPE is the Constant Phase Element.

The main parameters deduced from the analysis of Nyquist diagram for mild steel in 1 M HCl containing various concentrations of the investigated inhibitor is given in Table 1.

On increasing inhibitor concentration, the charge transfer resistance (R_{ct}) increased and the double layer capacitance (C_{dl}) decreased indicating that, the increasing inhibitor concentration decreased corrosion rate. Further inspection of the data presented in Table 1 shows that values of inhibition efficiency increased as the concentration of inhibitor increases. Decrease in the double layer capacitance was caused by reduction in local dielectric constant and/or by an increase in the thickness of the electrical double layer. This fact suggests that the inhibitor molecules acted by adsorption at the metal/solution interface [32]. On the other hand, the decrease

in the values of C_{dl} with an increase in the inhibitor concentration suggests an increase in the surface coverage by the inhibitor, which led to an increase in the inhibition efficiency. The decrease in the C_{dl} is in accordance with the Helmholtz model shown in the equation:

$$C_{dl} = \epsilon \epsilon_0 A d^{-1} \quad (11)$$

Where d is the thickness of the protective layer, ϵ is the dielectric constant of the medium, ϵ_0 is the vacuum permittivity and A is the effective area of the electrode. This model shows that C_{dl} is inversely proportional to the thickness of the protective layer meaning that the protective layer becomes thicker as the inhibitor concentration increases thus rendering the corrosion inhibition more effective [33].

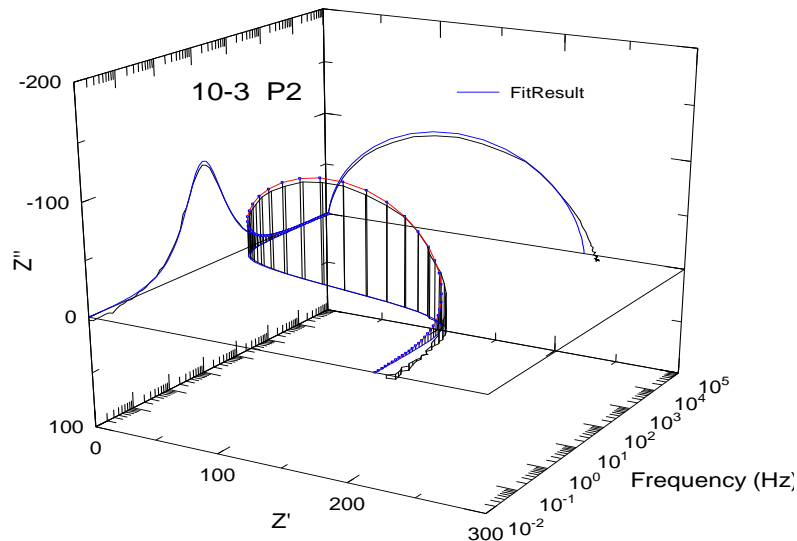


Figure 4: EIS Nyquist and Bode diagrams 3D for mild steel/1 M HCl + 10^{-3} M of **P2** interface: (---) experimental; (—) fitted data.

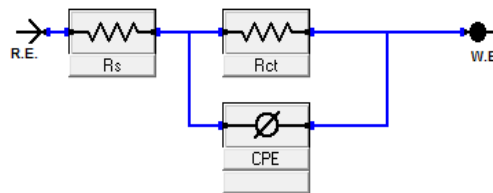


Figure 5: Equivalent circuit model used to fit the impedance spectra

Table 1: EIS parameters for the corrosion of mild steel in 1 M HCl solution containing different concentrations of P2 at 308 K.

Inhibitor	Concentration (M)	R_{ct} ($\Omega \cdot \text{cm}^2$)	R_s ($\Omega \cdot \text{cm}^2$)	CPE ($\mu\Omega^{-1} S^n \text{cm}^{-2}$)	n	C_{dl} (μF)	E_{Rct} (%)
1M HCl	--	14.50	1.93	393	0.88	200	--
P2	10^{-6}	57	1.72	773	0.91	45	75
	10^{-5}	77	1.75	695	0.89	43	81
	10^{-4}	192	1.82	619	0.92	40	92
	10^{-3}	219	1.94	554	0.93	37	93

The inhibition efficiency afforded by P2 may be attributed to the presence of electron rich S, N, O atoms and aromatic rings. One benzothiazine ring is common with the structure of both the inhibitor. Therefore, the possible coordinating centers are unshared electron pair of S, N, O and τ -electrons of aromatic rings.

3.2. Weight loss measurements

3.2.1. Effect of inhibitor concentration

The effect of addition of P2 tested at different concentrations on the corrosion of carbon steel in 1.0 M HCl solution was also studied by weight loss method at 308 K after 6 h of immersion period. The inhibition efficiency ($E_w\%$) were calculated by the following equation [34]:

$$E_w (\%) = \frac{W_0 - W_i}{W_0} \times 100 \quad (12)$$

Where w_0 and w_i are the weight loss values in the absence and presence of inhibitor.

Table 2: Corrosion parameters obtained from weight loss measurements of mild steel after 6h immersions in 1 M HCl solution with and without addition of various concentrations of benzothiazine derivatives P2 at 308k.

Inhibitor	Concentration (M)	V (mg.cm ⁻² .h ⁻¹)	E_w (%)	θ
1M HCl	-	0.82	---	---
P2	10 ⁻⁶	0.23	72	0.72
	10 ⁻⁵	0.14	83	0.83
	10 ⁻⁴	0.11	87	0.87
	10 ⁻³	0.05	94	0.94

Weight loss data of mild steel in 1 M HCl in the absence and presence of various concentrations of inhibitor is represented in Table 2. The calculated values of E_w of P2 indicate that E_w increases with the increasing P2 concentration showing a maximum E_w of 94% at 308 K at P2 concentration of 10⁻³M. The corrosion inhibition by P2 in 1 M HCl can be explained in terms of the adsorption of its molecules on the surface of mild steel. The adsorption of P2 is assumed to be a quasi-substitution process between water molecules on the steel surface and the P2 molecules. The adsorption of P2 on mild steel surface makes a barrier for mass and charge transfer, and consequently, mild steel is protected from aggressive acid solution. The increased E_w with the increasing P2 concentration indicates that more inhibitor molecules are adsorbed on the mild steel surface leading to the formation of a protective film [35-37]. Weight loss measurements also confirm the inhibiting nature of P2, and the $E_w(\%)$ values obtained from this method show the same trend as those obtained from the polarization and EIS techniques. The use of the benzothiazine as corrosion inhibitors have been widely reported by several authors [38-41].

3.2.2. Adsorption consideration and thermodynamic calculations

Basic information on the interaction between the inhibitor molecules and the metal surface could be provided from the adsorption isotherms. The experimental data were applied to different adsorption isotherm equations such as the Langmuir, Frumkin, Temkin and Freundlich. ‘Langmuir’ adsorption isotherms [42] were found to fit well with the experimental data.

The adsorption isotherm relationship of Langmuir is represented by the following equation [42, 44]:

$$\frac{C}{\theta} = \frac{1}{k} + C \quad (13)$$

Where C_{inh} is the inhibitor concentration, K_{ads} is the adsorption equilibrium constant and θ is the surface coverage (calculated from Eq. (13)). The relation between C_{inh}/θ and C_{inh} at 308K was shown in Figure 6 for P2. A linear relation can be found between C_{inh}/θ and C_{inh} with regression coefficients (R) 0.9999 for P2. The slope and the intercept were detected. The slope was near unity. The slope of the isotherm deviates from unity. This deviation may be explained on the basis of interaction between the adsorbed species on the metal surface by mutual repulsion or attraction [45]. The value of the adsorption-desorption equilibrium constant (K_{ads}) was 2.8610⁵ M⁻¹ for P2. The high values of K_{ads} for the studied inhibitor indicated stronger adsorption on the mild

steel surface in the investigated corrosive solution. The equilibrium constant of adsorption– desorption process (K_{ads}) is related to the standard free energy of adsorption process by the equation [46]:

$$\Delta G_{ads} = -RT\ln(55.5K) \quad (14)$$

Where 55.5 is the concentration of water expressed in mol dm^{-3} , R is the molar gas constant and T is the absolute temperature. The values of the standard free energy of adsorption were -42.43 kJ/mol for P2. The negative values of ΔG_{ads} indicate the spontaneity of the adsorption process and the stability of the adsorbed layer on the carbon steel surface [47]. Generally, the adsorption type is regarded as physisorption if the absolute value of ΔG_{ads} is in the range of 20 kJ mol^{-1} or lower. The inhibition behavior is attributed to the electrostatic interaction between the organic molecules and steel surface. When the absolute value of ΔG_{ads} is in the order of 40 kJ mol^{-1} or higher, the adsorption could be seen as chemisorption. In this process, the covalent bond is formed by the charge sharing or transferring from the inhibitor molecules to the metal surface [48, 49]. The obtained ΔG_{ads} value in the studied temperature (308K) is in the range of -40 kJ mol^{-1} , indicating, therefore, that the adsorption mechanism of the P2 onto mild steel in 1 M HCl solution is mainly due to chemisorption.

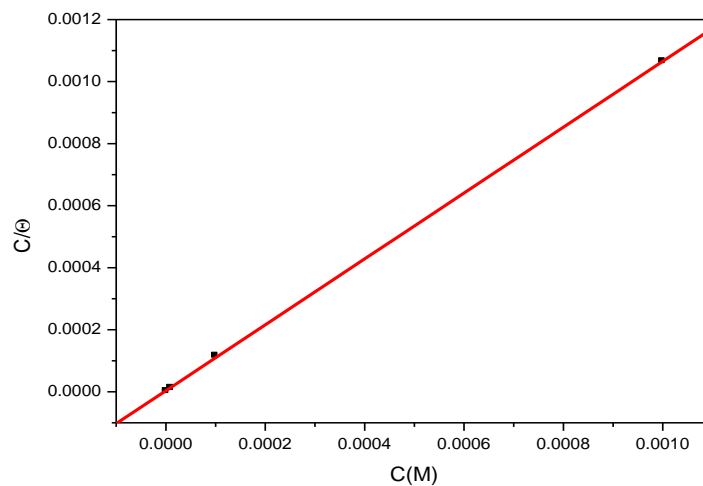


Figure 6: Langmuir adsorption isotherm for P2 on mild steel in 1 M HCl at 308K.

3.4. Potentiodynamic polarization measurements

Figure 7 shows the polarization curves of mild steel in 1 M HCl solution in the absence and presence of various concentrations (10^{-6} – 10^{-3} mol/l) of inhibitor P2 at 308K.

The nature of the polarization curves remains almost same in the absence and the presence of P2 but in the presence of investigated inhibitor the curves shifted toward the lower current density as compared to the blank. The shift in current density toward lower current density in the presence of inhibitor increases on increasing the concentration of the inhibitor P2.

In order to obtain information about the kinetics of the corrosion, some electrochemical parameters, i.e., corrosion potential (E_{corr}) and cathodic (β_c) Tafel slopes, corrosion current density (I_{corr}), coverage surfaces (θ) and the inhibition efficiency ($E_p\%$) were obtained from the Tafel extrapolation of the polarization curve. These parameters are summarized in Table 3. The dependence of the degree of surface coverage (θ) and the inhibition efficiency ($E_p\%$) on the concentration of the inhibitor were calculated using the following equations [50]:

$$E_p\% = (i_{corr(0)} - i_{corr(inh)}) / i_{corr(0)} * 100 \quad (15)$$

where $i_{corr(0)}$ and $i_{corr(inh)}$ represent corrosion current density values without and with inhibitor, respectively.

$$\Theta = E_p / 100 \quad (16)$$

The corrosion current density values were determined by the extrapolation of the linear portions of the anodic current–potential curves to the corresponding corrosion potentials (E_{corr}). The corrosion current density (I_{corr}) decreases in the presence of the studied P2 inhibitor compared to the blank solution, indicating that this inhibitor is adsorbed on the steel surface and inhibits the corrosion process.

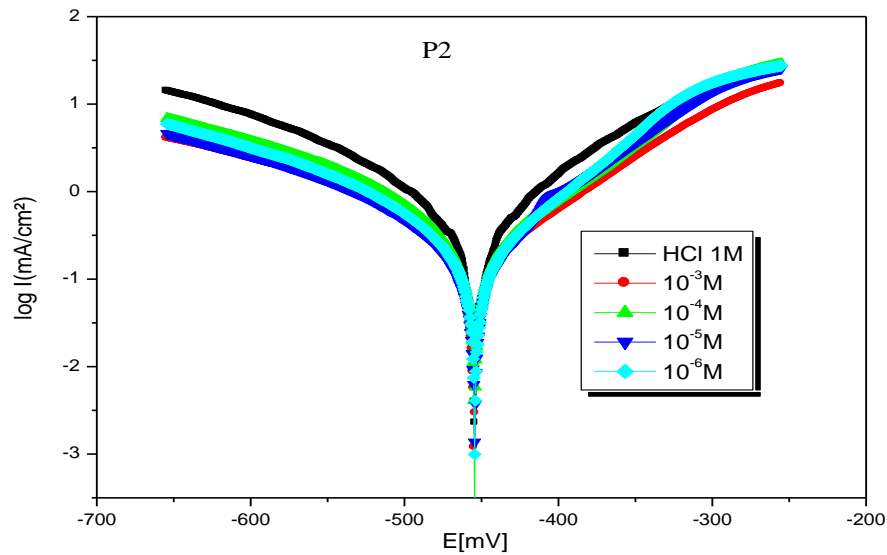


Figure 7: Polarisation curves of mild steel in 1M HCl at different concentrations of P2.

The potentiodynamic polarization curves in Figure 7 shows a reduction in anodic and cathodic currents in the presence of the tested inhibitor compared to the blank solution, that indicates the hydrogen evolution and dissolution metal were inhibited. Furthermore, the parallel variation of cathodic and anodic Tafel curves shows that the mechanism of inhibition in the presence of the investigated inhibitor is activation controlled, while the metal dissolution mechanism is not affected by the presence of P2 inhibitor [51].

Table 3: Values of electrochemical parameters evaluated from the cathodic current-voltage characteristics for the system electrode/1 M HCl with and without added inhibitor at 308 K.

Inhibitor	Concentration (M)	E_{corr} (mV/SCE)	I_{corr} ($\mu\text{A}/\text{cm}^2$)	β_c (V/dec)	E_p (%)	θ
1M HCl	--	-459	1381	-0.299	--	--
P2	10^{-6}	-442	474	-0.281	66	0.66
	10^{-5}	-461	293	-0.287	79	0.79
	10^{-4}	-453	152	-0.276	89	0.89
	10^{-3}	-455	99	-0.285	93	0.93

Examination of Table 3 shows that I_{corr} in 1 M HCl is very high indicating strong corrosiveness of mild steel in these acidic chloride media. In the presence of the inhibitor P2, the I_{corr} is seen to drop remarkably and the extent of reduction is found to be concentration dependent. As the inhibitor concentration increases, the I_{corr} decreases and the lowest value was obtained at concentration of 10^{-3} M.

According to data shown in Table 3, the inhibition efficiency increases with the increasing inhibitor concentration and were in the range of 66–93% within an accuracy of $\pm 0.5\%$ for P2. Increase in inhibition efficiency with increasing inhibitor concentration indicates that, more inhibitor molecules are adsorbed on the metal surface providing wider surface coverage and the compounds act as excellent adsorption inhibitor [52]. In 1 M HCl solution, the presence of P2 cause a negative shift in E_{corr} , which indicates that inhibitor molecules are

more adsorbed on the cathodic sites resulting in an inhibition of the cathodic reactions. However, the influence is more pronounced in the cathodic polarization plots compared to that in the anodic polarization plots. Generally, if the displacement in E_{corr} is >85 mV with respect to E_{corr} in uninhibited solution, the inhibitor can be seen as a cathodic or anodic type [53, 55]. Finally, the tested P2 inhibitor showed good inhibition efficiency for mild steel corrosion process in chloride containing acidic solution at the used concentrations.

3.5. Computational theoretical studies

The FMOs (HOMO and LUMO) are very important for describing chemical reactivity. The HOMO containing electrons, represents the ability (E_{HOMO}) to donate an electron, whereas, LUMO haven't not electrons, as an electron acceptor represents the ability (E_{LUMO}) to obtain an electron. The energy gap between HOMO and LUMO determines the kinetic stability, chemical reactivity, optical polarizability and chemical hardness–softness of a compound [56].

In this study, the HOMO and LUMO orbital energies were calculated using B3LYP method with 6-31G which is implemented in Gaussian 09 package [57-58]. All other calculations were performed using the results with some assumptions. The higher values of E_{HOMO} indicate an increase for the electron donor and this means a better inhibitory activity with increasing adsorption of the inhibitor on the metal surface, whereas the lower values of E_{LUMO} indicates the ability to accept electron of the molecule. The adsorption ability of the inhibitor to the metal surface increases with increasing of E_{HOMO} and decreasing of E_{LUMO} . The HOMO and LUMO orbital energies of the **P3** and **P4** inhibitors were performed and were given and shown in (Table 4) and (Figure 8), respectively. High ionization energy (> 6 eV) indicates high stability of **P3** and **P4** inhibitors [59]. The number of electrons transferred (ΔN), dipole moment, ionization potential, electron affinity, electronegativity, hardness, softness and total energy were also calculated and tabulated in (Table 4).

Table 4: Quantum chemical parameters for **P3** and **P4** obtained in gaseous and aqueous phases using the DFT at the B3LYP/6-31G level.

Parameter	Gas phase	Aqueous phase
Total Energy TE (eV)	-25957.4	-25957.6
E_{HOMO} (eV)	-6.6243	-6.7780
E_{LUMO} (eV)	-0.2174	-0.1747
Gap ΔE (eV)	6.4069	6.6033
Dipole moment μ (Debye)	2.8740	4.1011
Ionization potential I (eV)	6.6243	6.7780
Electron affinity A	0.2174	0.1747
Electronegativity χ	3.4208	3.4763
Hardness η	3.2034	3.3017
Electrophilicity index ω	1.8265	1.8301
Softness σ	0.3122	0.3029
Fractions of electron transferred ΔN	0.5586	0.5336

The value of ΔN (number of electrons transferred) show that the inhibition efficiency resulting from electron donation agrees with Lukovit's study [60]. If $\Delta N < 3.6$, the inhibition efficiency increases by increasing electron donation ability of these inhibitors to donate electrons to the metal surface [61]. Pertinent valence and dihedral angles, in degree, of the studied inhibitor calculated at B3LYP/6-31G(d,p) in gas and aqueous phases are given in the table 4.

Table 5 displays the most relevant values of the natural population ($P(N)$, $P(N-1)$ and $P(N+1)$) with the corresponding values of the Fukui functions (f_k^+ , f_k^- and f_k^0) of the studied inhibitors. The calculated values of the f_k^+ for inhibitors are mostly localized on the 1,4-benzothiazin-3(4H)-one ring, namely C_1 , C_3 , C_6 , O_{12} and S_{14} , indicating that the 1,4-benzothiazin-3(4H)-one ring will probably be the favorite site for nucleophilic attacks.

Table 5: Pertinent natural populations and Fukui functions of P2 calculated at B3LYP/6-31G in gas (G) and aqueous phases.

Atom k	Phase	$P(N)$	$P(N-1)$	$P(N+1)$	f_k^-	f_k^+	f_k^0
C_1	G	5,30898	5,44182	5,30969	0,1328	-0,0007	0,0661
	A	5,28847	5,45606	5,29322	0,1676	-0,0047	0,0814
C_3	G	6,2235	6,3148	6,1903	0,0913	0,0332	0,0623
	A	6,25815	6,34241	6,17851	0,0843	0,0796	0,0820
C_6	G	6,24245	6,34133	6,15693	0,0989	0,0855	0,0922
	A	6,25513	6,35183	6,16493	0,0967	0,0902	0,0934
O_{12}	G	8,60656	8,70747	8,48717	0,1009	0,1194	0,1102
	A	8,61229	8,74378	8,54751	0,1315	0,0648	0,0981
S_{14}	G	15,69509	15,79582	15,44529	0,1007	0,2498	0,1753
	A	15,67319	15,80763	15,41038	0,1344	0,2628	0,1986

The geometry of P2 in gas and aqueous phase (Figure 8) were fully optimized using DFT based on Beck's three parameter exchange functional and Lee–Yang–Parr nonlocal correlation functional (B3LYP) [62–64] and the 6–31G. The optimized structure shows that the molecule P2 has a non-planar structure. The HOMO and LUMO electrons density distributions of P2 are given in Table 6.

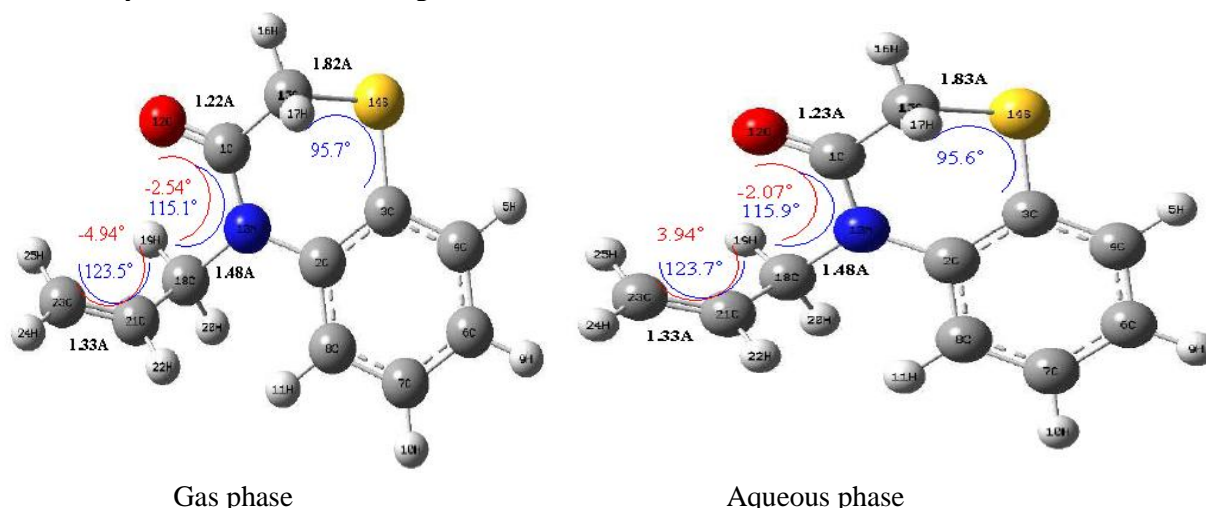
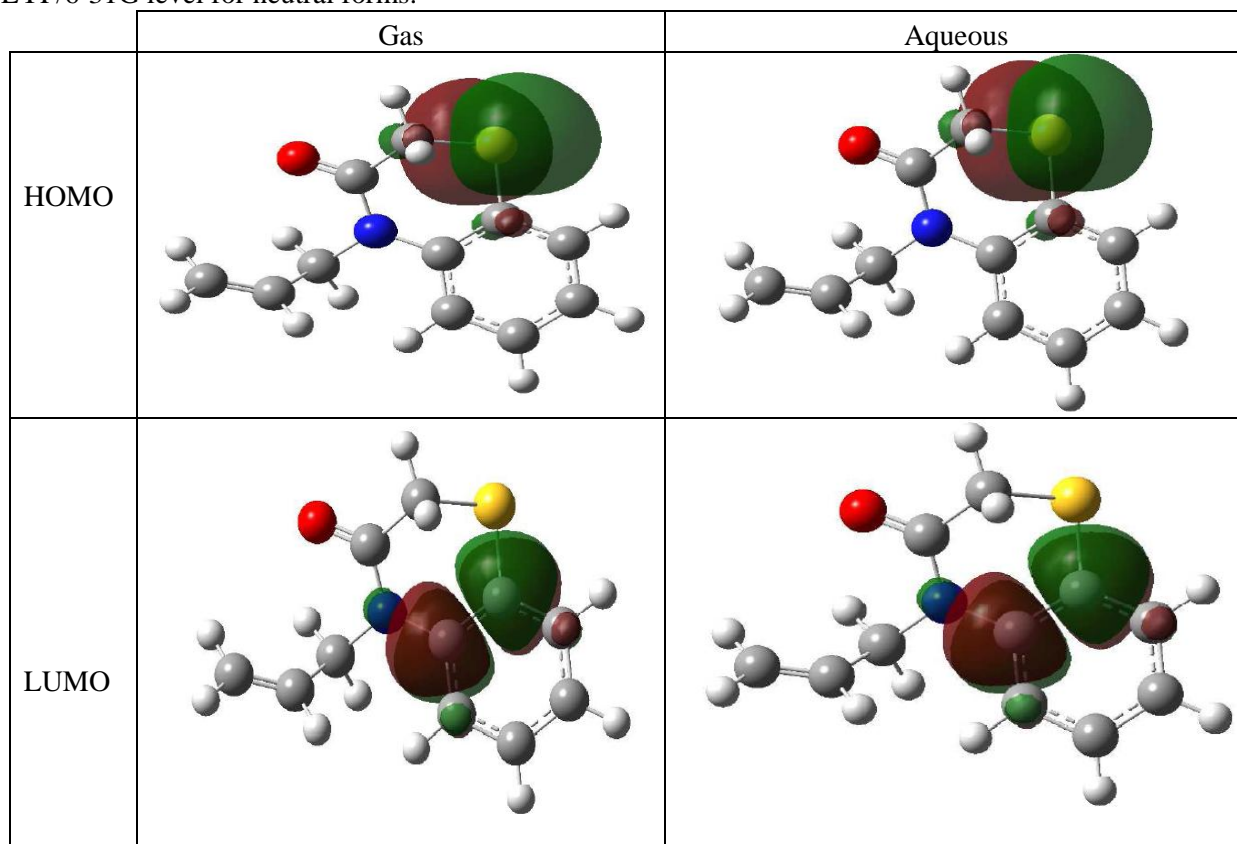


Fig. 8: Optimized molecular structures and selected dihedral angles (red), angles (blue) and bond lengths (black) of the studied inhibitors calculated in gaseous and aqueous phases using the DFT at the B3LYP/6-31G level.

As we know, frontier orbital theory is useful in predicting the adsorption centres of the inhibitors responsible for the interaction with surface metal atoms. Table 6 shows the HOMO and LUMO orbital contributions for the neutral studied inhibitor. The HOMO densities were concentrated on 1,4-benzothiazin-3(4H)-one ring.

Table 6: The HOMO and the LUMO electrons density distributions of P2 in gas and aqueous phase computed at B3LYP/6-31G level for neutral forms.



Conclusions

This paper describes the synthesis and characterization of 4-allyl-2H-1,4-benzothiazin-3(4H)-one (P2). The molecular structure of the compound has been determined by NMR spectroscopy. The corrosion inhibition of mild steel by the synthesized compound was studied by electrochemical and theoretical studies and the obtained results show that:

- ✓ The inhibition efficiency on mild steel in 1 M HCl solution increases with increasing the inhibitor concentration. The maximum inhibition efficiency of 93% was observed at 10^{-3} M of P2.
- ✓ The potentiodynamic polarization curves indicated that the inhibitor molecules are more adsorbed on the cathodic sites resulting in an inhibition of the cathodic reactions.
- ✓ EIS results showed that, the charge transfer resistance increases and the double layer capacitance decreases with increasing the inhibitor concentration.
- ✓ The adsorption of the inhibitor obeys the Langmuir adsorption isotherm via a strong chemical interaction with the mild steel surface.
- ✓ Finally, this study shows a good correlation between the theoretical and electrochemical data which confirms the reliability of quantum chemical methods to investigate the corrosion inhibition of metal surfaces.

Reference

1. Xia S., Qiu M., Yu L., Liu F., Zhao H., *Corros. Sci.* 50 (2008) 2021.
2. Larabi L., Harek Y., Benali O., Ghalem S., *Prog Org Coat.* 54 (2005) 256.
3. Behpour M., Ghoreishi S.M., Soltani N., Salavati-Niasari M., Hamadani M., Gandomi A., *Corros.Sci.* 50 (2008) 2172.
4. Awad M.K., Issa R.M., Atlam F.M., *Mater. Corros.* 60 (2009) 813.

5. Quraishi M.A., Sardar R., Jamal D., *Mater. Chem. Phys.* 71 (2001) 309.
6. Jamalizadeh E., Hosseini S.M.A., Jafari A.H., *Corros. Sci.* 51 (2009) 1428.
7. Gece G., Bilgic S., *Corros. Sci.* 51 (2009) 1876.
8. Gupta R., Ojha K. G., *Chem and Biochemical Aspects.* 4 (1988) 163-269.
9. Gowda J., Khader A. M. A., Kalluraya B., Shree P., Shabaraya A. R., *European Journal of Medicinal Chemistry.* 46 (2011) 4100-4106.
10. hairnar B. J., Salunke R. S., Patil P. B., Patil S. A., Kapade R. J., Girase P. S., Chaudhari B. R., *E-Journal of Chemistry.* 9(1) (2012) 318-322.
11. Sebbar N. K., Ellouz M., Essassi E. M., Ouzidan Y., Mague J. T., *Acta Cryst.* E71 (2015) o999.
12. Ellouz M., Sebbar N. K., Essassi E. M., Ouzidan Y., Mague J. T., *Acta Cryst.* E71 (2015) o1022-o1023.
13. Sebbar N. K., Ellouz M., Essassi E. M., Saadi M., El Ammari L., *Acta Cryst.* E71 (2015) o423-o424.
14. Fringuelli R., Milanese L., Schiaffella F., *Mini-Rev. Med. Chem.* 5 (2005) 1061-1073.
15. Warren B. K., Knaus E. E., *Eur. J. Med. Chem.* 22 (1987) 411-415.
16. Armenise D., Muraglia M., Florio M. A., De Laurentis N., Rosato A., Carrieri A., Corbo F., Franchini C., *Arch. Pharm. Chem. Life Sci.* 345 (2012) 407-416.
17. Jacquot Y., Bermont L., Giorgi H., Refouvelet B., Adessi L. G., Daubrosse E., Xicluna A., *Eur. J. Med. Chem.* 36 (2001) 127-136.
18. Munirajasekar D., Himaja M., Sunil M., *Int. Res. J. Pharm.* 2 (2011) 114-117.
19. Pearson R.G., *Inorg. Chem.* 27 (1988) 734-740.
20. Sastri V.S., Perumareddi J.R., *Corrosion.* 53 (1997) 617-622.
21. Elmsellem H., Nacer H., Halaimia F., Aouniti A., Lakehal I., Chetouani A., Al-Deyab S. S., Warad I., Touzani R., Hammouti B., *Int. J. Electrochem. Sci.* 9(2014)5328.
22. Elmsellem H., Basbas N., Chetouani A., Aouniti A., Radi S., Messali M., Hammouti B., *Portugaliae. Electrochimica. Acta.* 2 (2014) 77.
23. Udhayakala P., Rajendiran T. V., Gunasekaran S., *Chem. J.Biol. Phys. SCIA.* 2(3) (2012)1151-1165.
24. Roy R.K., Pal S., Hirao K., *J. Chem. Phys.* 110(1999)8236.
25. Singh A., Singh V.K., Quraishi M.A., Arab. J. Sci. Eng. 38 (2013) 85.
26. Umoren S.A., Solomon M.M., Eduok U.M., Obot I.B., Israel A.U., *J. Environ. Chem.Eng.* 2 (2014) 1048.
27. Cruz J., Pandiyan T., Ochoa E.G., *J. Electroanal. Chem.* 8 (2005) 583.
28. Feng Y., Chen S., Guo W., Zhang Y., Liu G., *J. Electroanal. Chem.* 602 (2007) 115-122.
29. Bentiss F., Jama C., Mernari B., El Attari H., El Kadi L., Lebrini M., Traisnel M., Lagrenee M., *Corros. Sci.* 51 (2009) 1628.
30. Tan Y.J., Bailey S., Kinsellal B., *Corros. Sci.* 38 (1996) 1545.
31. Sakunthala P., Vivekananthan S.S., Gopiraman M., Sulochana N., Vincent A.R., *J. Surfact. Deterg.* 16 (2013) 251.
32. Sorkhabi H.A., Shaabani B., Seifzadeh D., *Electrochim. Acta.* 50 (2005) 3446.
33. Yoo S.H., Kim Y.W., Chung K., Kim N.K., Kim J.S., *Ind. Eng. Chem. Res.* 52(2013)10880.
34. Ellouz M., Elmsellem H., Sebbar N. K., Steli H., Al Mamari K., Nadeem A., Ouzidan Y., Essassi E. M., Abdel-Rahaman I., Hristov P., *J. Mater. Environ. Sci.* 7(7) (2016)2482-2497.
35. Sikine M., Kandri Rodi Y., Elmsellem H., Krim O., Steli H., Ouzidan Y., Kandri Rodi A., Ouazzani Chahdi F., Sebbar N. K., Essassi E. M., *J. Mater. Environ. Sci.* 7(4) (2016)1386-1395.
36. Elmsellem H., Youssouf M. H., Aouniti A., Ben Hadd T., Chetouani A., Hammouti B., *Russian, Journal of Applied Chemistry.* 87(6) (2014) 744.
37. Elmsellem H., Harit T., AounitiA., Malek F., Riahi A., Chetouani A., Hammouti B., *Protection of Metals and Physical. Chemistry of Surfaces.* 51(5) (2015) 873.
38. Hjouji M. Y., Djedid M., Elmsellem H., Kandri Rodi Y., Ouzidan Y., Ouazzani Chahdi F., Sebbar N. K., Essassi E. M., Abdel-Rahaman I., Hammouti B., *J. Mater. Environ. Sci.*7(4)(2016)1425-1435.
39. Sikine M., Kandri Rodi Y., Elmsellem H., Krim O., Steli H., Ouzidan Y., Kandri Rodi A., Ouazzani Chahdi F., Sebbar N. K., Essassi E. M., *J. Mater. Environ. Sci.* 7 (4) (2016) 1386-1395.

40. Filali Baba Y., Elmsellem H., Kandri Rodi Y., Steli H., AD C., Ouzidan Y., Ouazzani Chahdi F., Sebbar N. K., Essassi E. M., Hammouti B., *Der Pharma.Chemica.* 8(4)(2016)159-169.
41. Hjouji M. Y., Djedid M., Elmsellem H., Kandri Rodi Y., Benalia M., Steli H., Ouzidan Y., Ouazzani Chahdi F., Essassi E. M., Hammouti B., *Der Pharma Chemica.* 8(4)(2016)85-95.
42. Elmsellem H., Elyoussfi A., Sebbar N. K., Dafali A., Cherrak K., Steli H., Essassi E. M., Aouniti A. and Hammouti B., *Maghr. J. Pure & Appl. Sci.*1 (2015) 1-10.
43. Elmsellem H., Aouniti A.,Khoutoul M., Chetouani A., Hammouti B., Benchat N., Touzani R. and Elazzouzi M., *J. Chem. Pharm. Res.* 6 (2014) 1216.
44. Elmsellem H., AounitiA., Youssoufi M.H., BendahaH., Ben hadda T., Chetouani A., Warad I., Hammouti B., *Phys. Chem. News.* 70 (2013) 84.
45. Elmsellem H., Elyoussfi A., Steli H., Sebbar N. K., Essassi E. M., Dahmani M., El Ouadi Y., Aouniti A., El Mahi B., Hammouti B., *Der Pharma Chemica.* 8(1) (2016) 248.
46. Aouniti A., Elmsellem H., Tighadouini S., Elazzouzi M., Radi S., Chetouani A., Hammouti B., Zarrouk A., *Journal of Taibah University for Science.* (2015). <http://dx.doi.org/10.1016/j.jtusci.2015.11.008>.
47. Sebbar N. K., Elmsellem H., Boudalia M., lahmidi S., Belleaouchou A., Guenbour A., Essassi E. M., Steli H., Aouniti A., *J. Mater. Environ. Sci.* 6 (11) (2015) 3034-3044.
48. Elmsellem H., Karrouchi K., Aouniti A., Hammouti B., Radi S., Taoufik J., Ansar M., Dahmani M., Steli H. and El Mahi B., *Der Pharma Chemica.* 7(10) (2015) 237-245.
49. Chakib I., Elmsellem H., Sebbar N. K., Lahmidi S., Nadeem A., Essassi E. M., Ouzidan Y., Abdel-Rahman I., Bentiss F., Hammouti B., *J. Mater. Environ. Sci.* 7(6) (2016) 1866-1881.
50. El Azzouzi M., Aouniti A., Tighadouin S., Elmsellem H., Radi S., Hammouti B., El Assyry A., Bentiss F., Zarrouk A. 221 (2016) 633-641
51. Elmsellem H., Elyoussfi A., Steli H., Sebbar N. K., Essassi E. M., Dahmani M., El Ouadi Y., Aouniti A., El Mahi B., Hammouti B., *Der. Pharma. Chemica.* 8(1) (2016) 248-256.
52. Filali Baba Y., Elmsellem H., Kandri Rodi Y., Steli H., AD C., Ouzidan Y., Ouazzani Chahdi F., Sebbar N. K., Essassi E. M., Hammouti B., *Der Pharma Chemica.* 8(4) (2016)159-169.
53. Ismaily Alaoui K., El Hajjaji F., A.Azaroual M., Taleb M., Chetouani A., Hammouti B., Abridgach F., Khoutoul M., Abboud Y., Aouniti A., Touzani R., *J. Chem. Pharmac. Research.* 6(7) (2014) 63-81.
54. Sebbar N. K., Elmsellem H., Boudalia M., lahmidi S., Belleaouchou A., Guenbour A., Essassi E. M., Steli H., Aouniti A., *J. Mater. Environ. Sci.* 6 (11) (2015)3034-3044.
55. Qachchachi F. -Z., Kandri Rodi Y., Elmsellem H., Steli H., Haoudi A., Mazzah A., Ouzidan Y., Sebbar N. K., Essassi E. M., *J. Mater. Environ. Sci.* 7 (8) (2016)2897-2907.
56. Govindarajan M., Karabacak M., *Spectrochim.Acta Part A Mol Biomol.Spectrosc.* 85 (2012)251-60.
57. Becke A.D., *J. Chem. Phys.* 98 (1993) 1372.
58. Ellouz M., Sebbar N. K., Elmsellem H., Steli H., Fichtali I., Mohamed Abdelahi M. M., Al Mamari K., Essassi E. M., Abdel-Rahaman I., *J. Mater. Environ. Sci.* 7 (8) (2016) 2806-2819.
59. El Adnani Z., Benjelloun A.T., Benzakour M., Mcharfi M., Sfaira M., Saffaj T., EbnTouhami M., Hammouti B., Al-Deyab S.S., Ebenso E.E., *Int. J. Electrochem. Sci.*9 (2014)4732 – 4746.
60. Lukovits I., Kalman E., Zucchi F., *Corrosion.* 57 (2001)3-7.
61. Zerga B., Hammouti B., Ebn Touhami M., Touir R., Taleb M., Sfaira M., Bennajeh M., ForssalInt I., *J. Electrochem. Sci.* 7(2012)471 – 483.
62. Chakib I., Elmsellem H., Sebbar N. K., Essassi E. M., Fichtali I., Zerzouf A., Ouzidan Y., Aouniti A., El Mahi B. and Hammouti B., *Der Pharma Chemica.* 8(2) (2016)380-391.
63. Lee C., Yang W., Parr R.G., *Phys. Rev. B.* 37 (1988) 785.
64. Essaghouani A. L., Elmsellem H., Ellouz M., El Hafi M., Boulhaoua M., Sebbar N. K., Essassi E. M., Bouabdellaoui M., Aouniti A. and Hammouti B., *Der Pharma Chemica.* 8(2) (2016)297-305.